BIOCHEMICAL PHARMACOLOGY 75 (2008) 1761–1773

available at www.sciencedirect.com

ScienceDirect

journal homepage: www.elsevier.com/locate/biochempharm

STI571/doxorubicin concentration-dependent switch for diverse caspase actions in CML cell line K562

Malgorzata Czyz *, *Justyna Jakubowska*, *Malgorzata Sztiller-Sikorska*

Department of Molecular Biology of Cancer, Medical University of Lodz, 6/8 Mazowiecka Street, 92-215 Lodz, Poland

ARTICLE INFO

Article history:
Received 7 January 2008
Accepted 5 February 2008

Keywords:
CML
Caspases
Differentiation
Doxorubicin
STI571

ABSTRACT

We examined the response of the apoptosis-reluctant CML cell line K562 to doxorubicin alone or in combination with the tyrosine kinase inhibitor STI571. We found that at clinically relevant concentrations, doxorubicin induced differentiation and senescence, but did not induce apoptosis. Doxorubicin induced G_2/M arrest and mitochondrial transmembrane potential dissipation. Interestingly, drug-induced differentiation could be diminished by caspase inhibitors. STI571 caused a graded response characterized by differentiation at low concentrations and apoptosis at higher. STI571 was not observed to induce senescence. Combination of STI571 and caspase inhibitors protected cells from apoptosis but did not influence differentiation. The diverse mode of action of both drugs contributed to the response observed during combination treatment. An additive effect on proliferation was obtained. The mechanisms contributing to inhibition of cellular proliferation were complex and strongly dependent on the applied drug concentrations. Differentiation or apoptosis were enhanced by combined treatment only in narrow ranges of concentrations. Conclusion: DOX and STI571 along diverse mechanisms contributed to elevated levels of activated caspases which might be then responsible for a switch from differentiation to apoptosis.

1. Introduction

The fusion kinase p210 Bcr-Abl is present in almost all cases of chronic myelogenous leukemia (CML). Bcr-Abl activates numerous cell signaling pathways, resulting in increased cell proliferation, arrested differentiation, and resistance to apoptosis induced by chemotherapeutics. Specific targeting of this well-defined causal agent of cancer led to the development of STI571 (imatinib mesylate, Gleevec®). It inhibits Bcr-Abl kinase activity by occupying its ATP-binding pocket [1]. STI571, due to the excellent hematologic and cytogenetic responses, is the first-line treatment for newly diagnosed CML [2]. However, at 5 years, 15–20% of patients develop some form of resistance and another 5% discontinue therapy because of toxicity [3,4]. Patients in more advanced phases of CML often fail to respond to STI571 monotherapy or relapse after transient remission. This has guided the way to the design of a second generation of targeted therapies [5], or to the development of combined treatment.

* *Corresponding author*. Tel.: +48 426784277; fax: +48 426784277.
E-mail address: mczyz@csk.umed.lodz.pl (M. Czyz).

Abbreviations: Ara-C, cytarabine, cytosine arabinoside; Bcl-X_L(B-cell leukemia/lymphoma extra long), anti-apoptotic protein; CML, chronic myelogenous leukemia; DAPI, 4,6-diamidino-2-phenylidole; $\Delta\Psi_m$, mitochondrial transmembrane potential; DMSO, dimethyl sulfoxide; DOX, doxorubicin; FITC, fluorescein isothiocyanate; GATA-1, transcription factor; GPA, glycophorine A; IC_{50}, concentration with 50% inhibitory effect; MAP, mitogen-activated protein; PBS, phosphate-buffered saline; PI, propidium iodide; SA-β-gal, senescence-associated β-galactosidase (activity); TMRE, tetramethylrhodamine ethyl ester; zDEVD-fmk, *N*-benzyloxycarbonyl-Asp(OCH_3)-Glu(OCH_3)-Val-Asp(OCH_3)-fluoromethylketone; zVAD-fmk, *N*-benzyloxycabonyl-Val-Ala-Asp-fluoromethylketone.

0006-2952/$ – see front matter
doi:10.1016/j.bcp.2008.02.004

Numerous studies were performed to investigate the combined effects of STI571 and anticancer drugs on CML cells. Most combinations found to be either synergistic as with Ara-C [6], MEK1/2 inhibitor PD184352 [7], etoposide [8], As_4S_4 [9], arsenic trioxide [10], or additive as with daunorubicin or interferon-alpha [6]. There were also reports about antagonistic effects as with hydroxyurea [6]. The basis for these studies is the premise that inhibition of Bcr-Abl activity would sensitize the CML cells to the induction of apoptosis by conventional agents and extend the inhibition of cell proliferation to a broader population of CML cells reducing in this way the level of minimal residual disease.

Doxorubicin (DOX) is an interesting candidate for the combined therapy due to its well-defined mode of action [11,12]. It is not applied against CML mainly because it fails to induce apoptosis. Using human K562 cell line, a well-characterized model system for Bcr-Abl-positive CML, we concentrated on the question how these cells would respond to clinically relevant concentrations of DOX when Bcr-Abl activity was gradually reduced by using various concentrations of its inhibitor, STI571. We investigated the effects of these two drugs on (i) proliferation and distribution of cells in cell cycle; (ii) induction of erythroid-like differentiation measured by hemoglobin synthesis and γ-globin expression; (iii) induction of apoptosis visualized by morphological changes, mitochondrial transmembrane potential ($\Delta\Psi_m$) dissipation and externalization of phosphatidylserine; and (iv) induction of cellular senescence. An additive inhibitory effect on proliferation was observed. Differentiation or apoptosis were enhanced by combined treatment only in narrow ranges of concentrations.

Several recent publications described non-apoptotic functions of caspases including stimulation of differentiation [13–16]. The hypothesis has been presented that biochemical pathways of apoptosis are integral components of cell differentiation [17]. In light of those hypotheses we asked the question whether caspase activation which can occur in response to various extracellular and intracellular insults, might be the common causal agent of K562 cell differentiation stimulated by so diverse drugs as STI571 and DOX. For that we explored whether STI571- and DOX-induced differentiation involved mitochondria and caspase-dependent apoptotic machinery.

2. Materials and methods

2.1. Drugs

Doxorubicin was kindly provided by Dr. Irena Oszczapowicz and Mrs. Malgorzata Wasowska from the Institute of Biotechnology and Antibiotics, Warsaw. STI571 (imatinib mesylate; Novartis Pharmaceuticals, Basel, Switzerland) was a gift of Prof. Janusz Blasiak. Stock solutions (1 mM) of each compound, DOX in sterile water and STI571 in DMSO, were stored in the dark at −20° and diluted in RPMI 1640 medium immediately before use.

2.2. Cell culture conditions, cell viability and proliferation assay

The Bcr-Abl-positive human K562 cell line was maintained as described previously [18]. Cell proliferation and viability were determined by using Trypan blue dye exclusion assay (Sigma–Aldrich, St. Louis, MO, USA). For estimation of growth rate, treatment with drugs was carried out up to 4 days and aliquots were removed daily for determination of cell number.

2.3. Analysis of drug combination effects on proliferation

The median effect principle was used to analyze concentration-response data for single drug or drug combination which takes into account both the potency (D_m or IC_{50}) and the shape of the concentration–effect curve (the m value) [19]. First, IC_{50} values were determined to choose a constant drug concentration ratio. Then, concentration–effect and median–effect plots were constructed. Linear correlation coefficient (r) values were calculated. They were greater than 0.9 indicating that the data were applicable to the median effect principle and qualified for the analysis. Combination index (CI) values were calculated based on the formula: $d_{DOX}/D_{DOX} + d_{STI571}/D_{STI571}$, where D_{DOX} and D_{STI571} were the concentrations of DOX and STI571 alone required to produce x% effect, and d_{DOX} and d_{STI571} were the concentrations of drugs in combination which were iso-effective. D_{DOX} and D_{STI571} were calculated from the median–effect equation: $D = D_m[f_a/(1 - f_a)]^{1/m}$, where D_m was the median–effect concentration that was obtained from the anti-log of x-intercept of median effect plot, f_a was the fraction of the cells affected by the concentration C, and m was the slope of the median–effect plot [20]. CI values between 0.8 and 1.2 were defined as additive effect.

2.4. Benzidine staining

The benzidine oxidation test was performed as described previously [18]. Briefly, K562 cells were seeded at 4×10^4 ml^{-1} and 24 h later drugs alone or in combination were added. On day 4, 200 cells were counted for each sample to determine the percentage of benzidine-positive cells. In selected experiments, cells were seeded as above and 24 h later culture medium was supplemented with one of caspase inhibitors, zVAD-fmk (Promega, Madison, WI, USA) or zDEVD-fmk (BD Pharmingen, CA, USA), to the final concentrations of 40 μM or with DMSO (0.2%). 30 min later, DOX or STI571 were added at the indicated concentrations and benzidine staining was assessed on day 4.

2.5. Quantitative real-time reverse transcription PCR

Total RNA and cDNA were prepared as described before [21]. Amplification reactions were performed in a final volume of 20 μl using qPCR™ Core Kit with Sybr™ Green I w/o dUTP (EUROGENTEC, Seraing, Belgium), 300 nM primers and 25 ng DNA template per reaction. The following primers were used: for γ-globin: 5′-CCA TAA AGC ACC TGG ATG ATC-3′ and 5′-ATC TGG AGG ACA GGG CAC TG-3′, RPS17: 5′-TCG CTT CAT CAG ATG CGT GAC ATA ACC TG-3′ and 5′-AAG CGC GTG TGC GAG GAG ATC G-3′, β-microglobulin: 5′-TGA GTG CTG TCT CCA TGT TTG A-3′ and 5′-TCT GCT CCC CAC CTC TAA GTT G-3′. Gene expression levels of γ-globin, RPS17, and β-microglobulin were tested using the Rotor-Gene 3000 real-time DNA analysis system (Corbett Research, Australia). The relative expression was based on the expression ratio of the target gene (γ-globin)

versus a reference gene (RPS17 and β-microglobulin). To calculate the relative gene expression ratios of single samples a mathematical model was used which included an efficiency correction for real-time PCR efficiency of the individual transcripts [22].

2.6. Acridine orange/ethidium bromide staining

Cell death was studied morphologically using fluorescent dyes: acridine orange (AO) and ethidium bromide (EB). Briefly, the cells were cultured for 2 or 3 days with or without tested drugs at indicated concentrations. Cells (1×10^5) were collected by centrifugation and resuspended in 100 μl of cold PBS. 20 μl of staining solution (1:1) mixture of 100 μg/ml of EB and 100 μg/ml of AO (Sigma Chemical Co.) was added. Then, they were examined by ultraviolet fluorescence microscopy (Olympus BX 41). In each experiment, more than 200 cells were analyzed and then percentages of early/late apoptotic or necrotic cells were calculated.

2.7. Flow cytometry

All stained cells were analyzed using the standard optics of a FACSCalibur flow cytometer (Becton Dickinson, San Jose, CA). Cell cycle analysis was performed on propidium iodide (PI; BD Pharmingen, San Diego, CA, USA)-stained cells after 2 days of treatment with increasing concentrations of STI571 and/or 40 nM DOX. The percentages of the cell population in subG_1, G_1, S or G_2/M phases were calculated from histograms using the CellQuest software (BD Sciences, San Jose, CA). To assess apoptosis dual staining of cells with Annexin V and PI was used. After drug treatment for 2 days, 1×10^5 cells were washed in cold PBS and resuspended in 200 μl staining solution containing 5 μl of Annexin V-fluorescein isothiocyanate (FITC) and 10 μl of 20 μg/ml PI (Roche Diagnostics, Mannheim, Germany). To monitor changes in $\Delta\Psi_m$, drug-treated or untreated cells were loaded with tetramethylrhodamine ethyl ester (TMRE) (Molecular Probes, Invitrogen, Eugene, OR, USA) at 100 nM, 37 °C for 20 min. To relate differentiation with caspase activation double staining for glycophorine A (CD235a; GPA) and caspase-3 activation was performed. Anti-human PE-conjugated mouse monoclonal antibody to the GPA antigen (Caltag™ Laboratories, Invitrogen Corporation, USA) for detecting differentiation marker and a fluorogenic NucView™ 488 Caspase-3 substrate (Biotium, Inc., Hayward, CA, USA) for detecting caspase-3 activity were used. Briefly, 1.2×10^5 untreated or 100 nM DOX-treated K562 cells were first washed and incubated with 3 μl of NucView™ for 20 min at room temperature, then cells were washed twice with PBS containing 2% of FBS and 5 μl of antibody to GPA was added. After incubation for 15 min at room temperature, cells were washed, resuspended in PBS containing 2% FBS, and analyzed by flow cytometry.

2.8. Senescence assay

β-Galactosidase staining (Senescent Cells Staining Kit, Sigma–Aldrich, Israel) was used to quantify senescence in DOX and/or STI571 treated cells. In selected experiments, caspase inhibitor, zVAD-fmk (Promega, Madison, WI, USA) was added to the culture treated with 60 or 100 nM DOX. Briefly, cells were washed twice with PBS and fixed with 2% formaldehyde, 0.2% glutaraldehyde for 6 min. The cells were then washed again with PBS and stained with a solution containing 5-bromo-4-chloro-3-indolyl-β-D-galactopyranoside (X-gal), as described by manufacturer. Following overnight incubation at 37 °C with no CO_2, cells were washed with PBS, and the percentage of positively stained cells was determined after counting about 200 cells in random fields. Representative microscopic fields (Olympus CKX41) were photographed.

2.9. Detecting caspase-3 activity within living cells

K562 cells were treated with DOX or STI571 alone or in combination for 4 days. A fluorogenic NucView™ 488 Caspase-3 substrate (Biotium, Inc., Hayward, CA, USA) was used for detecting caspase-3 activity within cells. Briefly, to 1×10^5 cells in 0.2 ml PBS 5 μl of 0.2 mM NucView™ 488 Caspase-3 substrate stock solution was added. After 15 minutes of incubation at room temperature cells were centrifuged and resuspended in 20 μl PBS. Cells with green stained nuclei were observed on a slide under a fluorescence microscope. As a negative control untreated cells and as a positive control cells treated with 1 μM STI571 were used. To some samples of DOX-induced cells, caspase-3 inhibitor Ac-DEVD-CHO was added 15 minutes prior to NucView™ 488 Caspase-3 substrate.

2.10. Statistical analysis

The data are expressed as means ± S.D. Subsequent analysis was done using Student-*t* test. Results were considered as significant when $p < 0.05$.

3. Results

3.1. Growth inhibitory effects of STI571 and DOX on K562 cell line are additive

To compare the effects of DOX and STI571, K562 cells were incubated with varying concentrations of drugs for 4 days. Viability was significantly reduced in cultures treated with 500 nM STI571 used alone or in combination with 40 nM DOX (Fig. 1A). 250 nM or lower concentrations of STI571 left more than 90% cells alive for 3 days. In combination treatment with 40 nM DOX, 250 nM STI571 was sufficient to significantly decrease cell viability. DOX alone did not markedly affect cell viability even in the presence of 100 nM (not shown). A duration-dependent reduction of cell proliferative capacity was observed in K562 cells treated with STI571 alone or in combination with 40 nM DOX. IC_{50} values of STI571 and DOX alone measured at day 3 were about 200 nM and 20 nM, respectively (Fig. 1B). The combined effects of STI571 and DOX on proliferation were examined at a constant ratio 10:1. The median–effect principle was applied to analyze the nature of drug interactions at various proliferation inhibition levels. The Fa–CI plot shown in Fig. 1B indicates additive effects up to Fa = 0.85 inhibition.

3.2. *Combined treatment with STI571 and DOX arrests K562 cells either in G_1 or in G_2/M depending on drug concentrations*

The effects of STI571 and DOX alone and in combination on the cell cycle distribution of K562 cells were evaluated after 2 days of treatment (Fig. 2). As previously shown [9,18], STI571 caused cell cycle arrest in G_1 phase, whereas 40 nM DOX accumulated K562 cells in G_2/M phase. Interestingly, after combined treatment with STI571 and 40 nM DOX, K562 cells were arrested either in G_1 or in G_2/M phase depending on STI571 concentrations. In addition, an increased accumulation in subG_1 was observed with increased STI571 concentrations. Flow cytometric analysis of changes in cell morphology

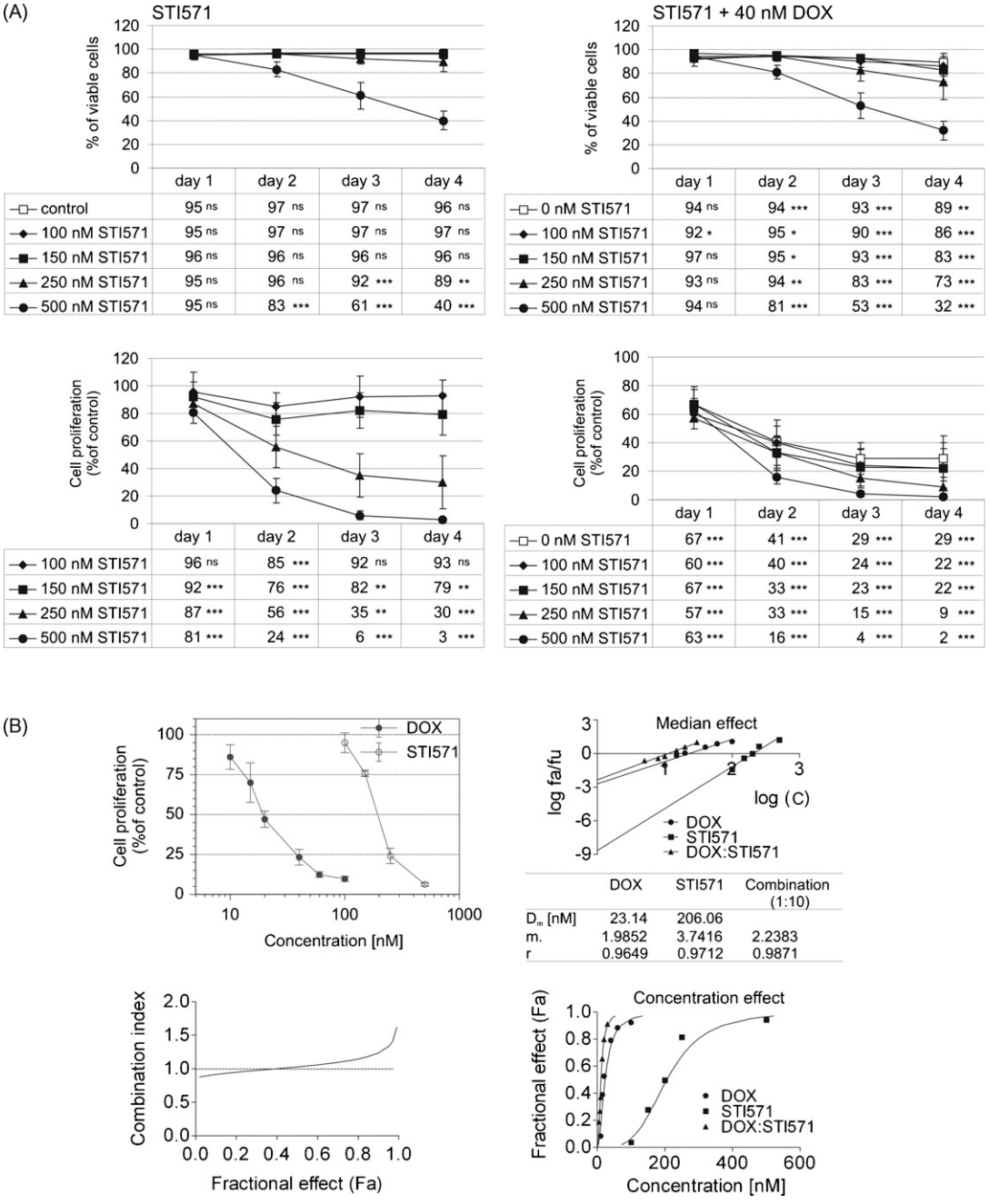

	day 1	day 2	day 3	day 4
control	95 ns	97 ns	97 ns	96 ns
100 nM STI571	95 ns	97 ns	97 ns	97 ns
150 nM STI571	96 ns	96 ns	96 ns	96 ns
250 nM STI571	95 ns	96 ns	92 ***	89 **
500 nM STI571	95 ns	83 ***	61 ***	40 ***

	day 1	day 2	day 3	day 4
0 nM STI571	94 ns	94 ***	93 ***	89 **
100 nM STI571	92 *	95 *	90 ***	86 ***
150 nM STI571	97 ns	95 *	93 ***	83 ***
250 nM STI571	93 ns	94 **	83 ***	73 ***
500 nM STI571	94 ns	81 ***	53 ***	32 ***

	day 1	day 2	day 3	day 4
100 nM STI571	96 ns	85 ***	92 ns	93 ns
150 nM STI571	92 ***	76 ***	82 **	79 **
250 nM STI571	87 ***	56 ***	35 **	30 ***
500 nM STI571	81 ***	24 ***	6 ***	3 ***

	day 1	day 2	day 3	day 4
0 nM STI571	67 ***	41 ***	29 ***	29 ***
100 nM STI571	60 ***	40 ***	24 ***	22 ***
150 nM STI571	67 ***	33 ***	23 ***	22 ***
250 nM STI571	57 ***	33 ***	15 ***	9 ***
500 nM STI571	63 ***	16 ***	4 ***	2 ***

	DOX	STI571	Combination (1:10)
D_m [nM]	23.14	206.06	
m	1.9852	3.7416	2.2383
r	0.9649	0.9712	0.9871

Fig. 1 – The effect of STI571 used alone or in combination with DOX on K562 cell viability and proliferation. (A) Cell cultures were treated with various concentrations of STI571 alone or in combination with 40 nM DOX for up to 4 days. The number of viable cells is expressed as percentage of total cell number. Cell proliferation is expressed as the percentage of cell number in control culture. Data represent the means and standard deviation of 6 independent experiments. (B) K562 cells were exposed to varying concentrations of DOX and STI571 for 3 days at a fixed ratio (1:10) which was chosen after determination of IC_{50}. Based on concentration–effect plots and median–effect plots, concentration–effect relationship parameters (D_m, m and r) and combination index (CI) values for proliferation were determined in relation to the fraction affected (Fa) as described in Section 2. CI values between 0.8 and 1.2 correspond to an additive interaction.

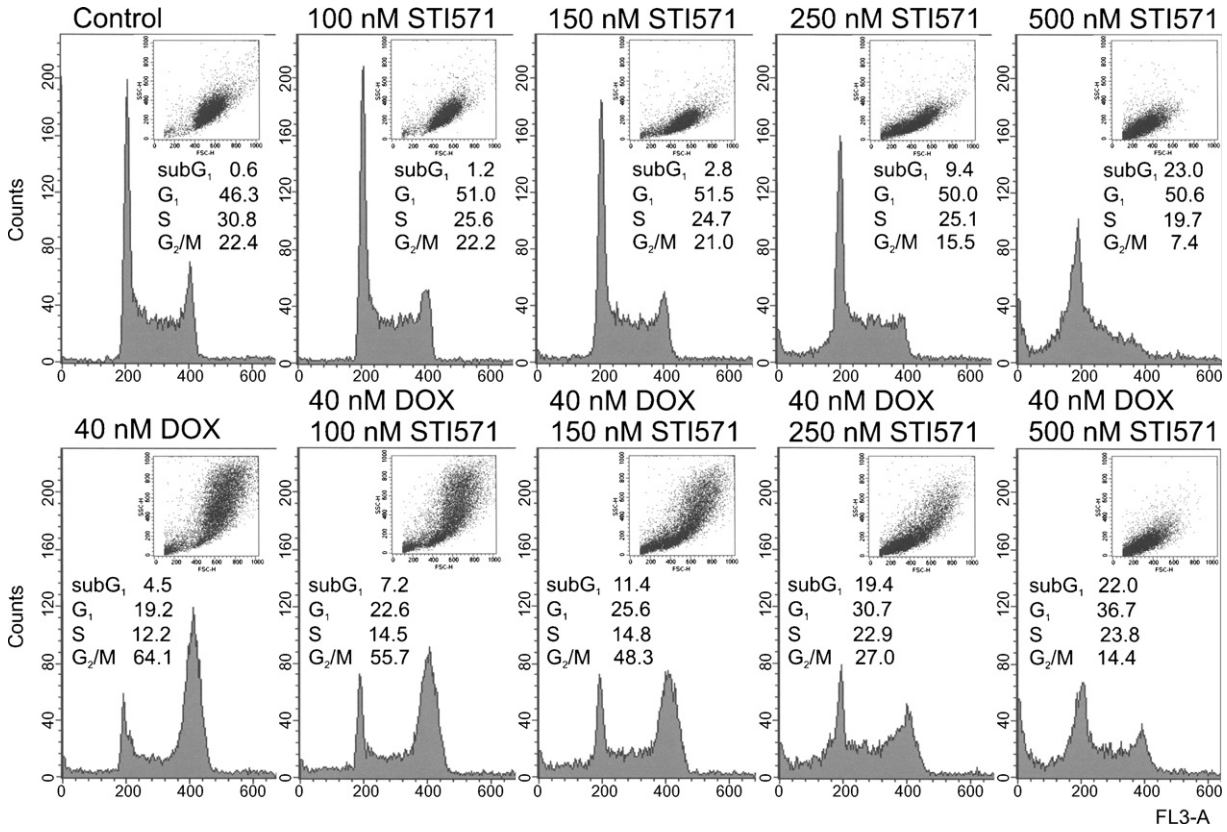

Fig. 2 – Diverse effects of STI571 and/or 40 nM DOX on cell cycle distribution, cell size and granularity. K562 cells were treated with various concentrations of STI571 and 40 nM DOX, either alone or in combinations as indicated. DNA contents were measured by flow cytometry on day 2 post-treatment as described in Section 2. Histograms present one out of 3 independent experiments.

(inserts in Fig. 2) revealed that G_2/M arrest caused by 40 nM DOX was connected to an increase in cell size and granularity, whereas STI571 induced opposite effects.

3.3. *Combined treatment with STI571 and DOX enhances cell differentiation in a narrow range of concentrations*

Induction of cell differentiation can cause inhibition of cell proliferation without cytotoxic effects. Erythroid-like differentiation of K562 cells was assessed by benzidine staining for hemoglobin synthesis and quantitative real-time PCR for erythroid gene expression. STI571 at the concentration of 150 nM, and DOX at the concentration of 60 nM induced appearance of about 20% hemoglobin-producing K562 cells (Fig. 3). DOX alone at higher concentrations caused further increase in the percentage of differentiated cells, whereas STI571 did not. Combined treatment enhanced differentiation in a very narrow range of low concentrations of both drugs. The optimal concentrations of STI571 and DOX used in combined treatment were 100–150 and 10–20 nM, respectively.

When γ-globin mRNA levels were assessed by quantitative real-time PCR, a similar concentration-dependence was observed as estimated by benzidine staining. The highest increase was observed in cultures stimulated with 150 nM STI571 (5.8-fold increase; $p < 0.01$) or 100 nM DOX (5.8-fold increase; $p < 0.001$). Combination of 15 nM DOX with 150 nM STI571 caused 5.3-fold increase ($p < 0.01$) in γ-globin mRNA level in comparison to the control level.

3.4. *Induction of apoptosis in K562 cells by low concentrations of STI571 is enhanced by DOX*

Bcr-Abl-expressing leukemic cells are highly resistant to apoptosis induced by chemotherapeutic agents. K562 cells were assessed for evidence of apoptotic cell death by different criteria: (i) morphological characteristics of apoptotic and necrotic cells after staining with acridine orange and ethidium bromide (day 2 and 3); (ii) translocation of phosphatidylserine to the outer plasma membrane by Annexin V staining (day 2); (iii) subdiploid DNA content by propidium iodide staining (day 2), and (iv) loss of mitochondrial transmembrane potential ($\Delta\Psi_m$) (days 1–4). DOX alone did not induce apoptosis of K562 cells (Fig. 4, Table 1). Neither Annexin V-staining nor double staining with acridine orange and ethidium bromide (AO/EB) for early and late apoptosis showed an enhancement of apoptosis after 2 or 3 days of treatment with DOX. Combined treatment of K562 cells with STI571 and DOX markedly enhanced apoptosis but only in a narrow range of STI571 concentrations. Combining 40 nM DOX with 250 nM or 500 nM STI571 almost doubled the increase in the number of apoptotic cells in comparison to STI571 alone when externalization of phosphatidylserine was assayed on day 2. Similar results were

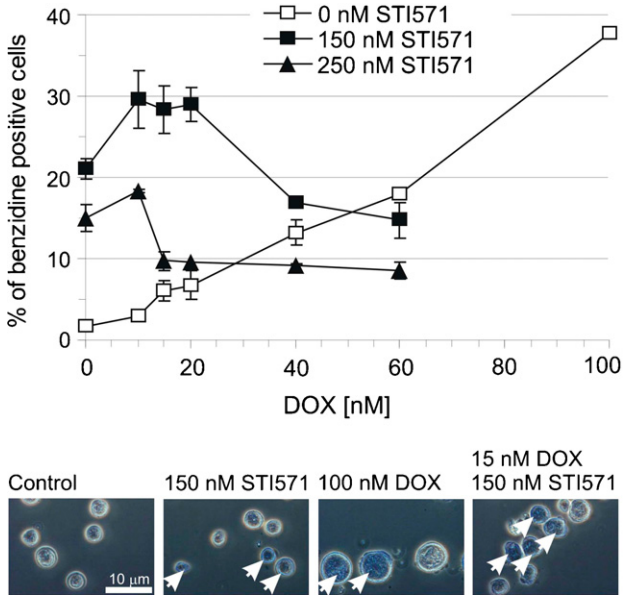

Fig. 3 – Combined treatment with STI571 and DOX enhances K562 cell erythroid-like differentiation in a narrow range of low concentrations. Effect of DOX in combination with STI571 on differentiation of K562 cells was assayed by benzidine staining on day 4 post-treatment with DOX and STI571 at selected concentrations. Data represent means and standard deviation of 4 independent experiments. Statistical analysis performed using two-tailed *t*-test indicated significant differences ($p < 0.001$) in relation to untreated cells for all treatment conditions except for DOX in the concentration range 10–20 nM where $p < 0.01$. Representative microscopic fields are shown for some experimental conditions. Arrows indicate some examples of cells stained blue. (For interpretation of the references to color in this figure legend, the reader is referred to the web version of the article.)

obtained when apoptosis was evaluated by assessment of subdiploid DNA content after staining with propidium iodide (subG$_1$ fraction in Fig. 2). When apoptosis was assessed on day 3, the stronger combined effects in comparison with single drug effects were already visible in cells treated with 150 nM STI571 and 40 nM DOX (Table 1, Fig. 4B). In summary, DOX enhanced STI571-induced apoptosis when STI571 was used in the range of 150–500 nM. At higher concentrations, this drug might be predominantly responsible for induction of apoptosis in K562 cells. It is also important to note that the necrosis levels were very low in all tested conditions (Table 1).

3.5. *DOX but not STI571 induces senescence in K562 cells*

Enlarged phenotype of cells treated with DOX prompted us to determine whether senescence was induced in K562 cells. SA-β-galactosidase (SA-β-gal) activity was present in cells already after 3 days of exposure to 40 nM DOX (Fig. 5A). Treatment with 100 nM DOX resulted in about 77% stained cells. A prolonged incubation with 100 nM DOX further increased the percentage of SA-β-gal-positive cells (about 83% on day 4, not shown). Cells expressing the senescence marker were larger in size (Fig. 5B), and showed a permanent growth arrest while maintaining viability, all of which are features indicative of senescence phenotype. STI571 did not induce senescence in K562 cells and caused a decrease in the percentage of SA-β-gal stained cells when used in combination with DOX. This indicates that induction of apoptosis by STI571 might inhibit DOX-induced senescence program.

3.6. *Both STI571 and DOX cause changes in mitochondria transmembrane potential*

We assessed loss of mitochondrial transmembrane potential ($\Delta\Psi_m$) in K562 cells treated with STI571 and/or DOX. Figs. 6 and 7A show representative histograms of TMRE fluorescence. Three cell populations could be distinguished. Population A consisted of cells with high TMRE fluorescence ($>2 \times 10^2$). The lowest $\Delta\Psi_m$ (population C) might arise from dead cells which

Table 1 – Dual staining with acridine orange and ethidium bromide indicates an enhancement in apoptosis but not necrosis after 2 and 3 days of combined treatment of K562 cells with low concentrations of STI571 and DOX

	Day 2			Day 3		
	Early apoptosis	Late apoptosis	Necrosis	Early apoptosis	Late apoptosis	Necrosis
Control	1.3 ± 0.6	0.3 ± 0.4	1.4 ± 0.3	0.8 ± 0.1	0.4 ± 0.1	0.3 ± 0.4
40 nM DOX	1.7 ± 0.7	1.3 ± 1.8	2.5 ± 0.4	5.9 ± 3.9	1.5 ± 1.2	1.7 ± 0.8
100 nM DOX	1.6 ± 1.0	1.9 ± 1.0	2.4 ± 0.8	1.8 ± 1.0	1.5 ± 0.6	**1.7 ± 0.1***
150 nM STI571	3.7 ± 1.3	1.1 ± 1.0	0.9 ± 0.6	6.4 ± 4.7	**2.5 ± 0.2****	0.9 ± 0.6
250 nM STI571	**26.3 ± 1.3****	**5.0 ± 0.8***	1.3 ± 0.1	**41.7 ± 11.3***	4.7 ± 2.1	0.5 ± 0.4
500 nM STI571	**57.1 ± 3.2****	**10.0 ± 3.8***	1.2 ± 0.9	66.3	18.4	0.2
40 nM DOX 150 nM STI571	11.4 ± 3.4	3.0 ± 1.9	1.3 ± 0.6	**31.3 ± 4.5***	6.3 ± 2.3	0.8 ± 0.4
40 nM DOX 250 nM STI571	**33.5 ± 1.1****	**4.7 ± 0.3****	1.9 ± 0.5	**49.7 ± 7.1***	16.4 ± 7.4	0.9 ± 0.1
40 nM DOX 500 nM STI571	**60.0 ± 6.6****	12.6 ± 7.4	0.5 ± 0.6	**55.0 ± 1.8****	**34.2 ± 4.3****	0.0 ± 0.0
100 nM DOX 150 nM STI571	6.9 ± 6.2	2.8 ± 1.5	1.8 ± 0.5	**29.7 ± 0.6****	7.1 ± 3.1	2.1 ± 0.9

A minimal of 200 cells was counted in each experiment and all four cellular states were recorded. Then, the percentages of early or late apoptotic or necrotic cells were calculated. Data represent means (±S.D.) of 2 independent experiments except for culture treated with 500 nM STI571 analyzed on day 3 when only one experiment was done. Bold data points marked with asterisks indicate significant differences ($^{*}p < 0.05$; $^{**}p < 0.01$) from the control data points.

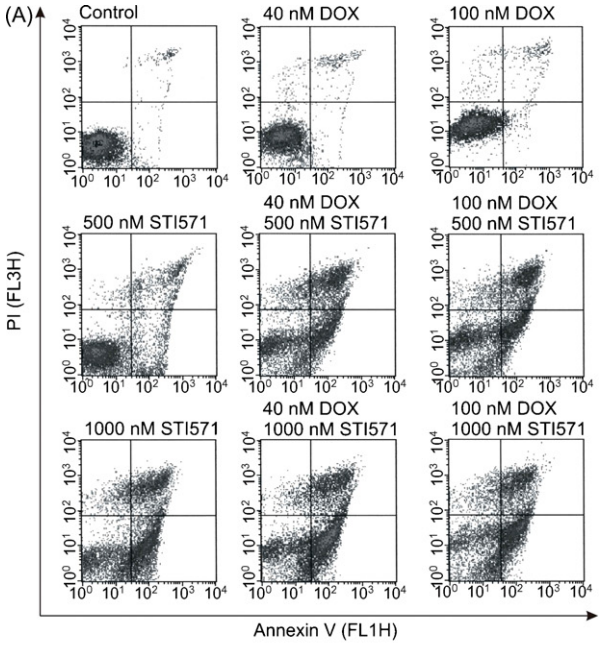

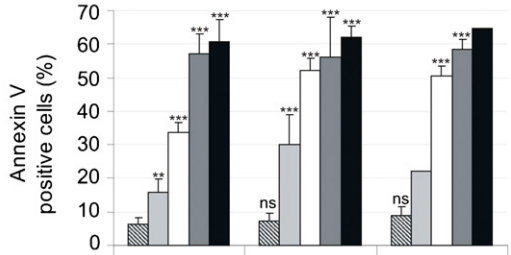

	0 nM DOX	40 nM DOX	100 nM DOX
0 nM STI571	6	7	9
250 nM STI571	16	30	22
500 nM STI571	34	52	51
800 nM STI571	57	56	58
1000 nM STI571	61	62	65

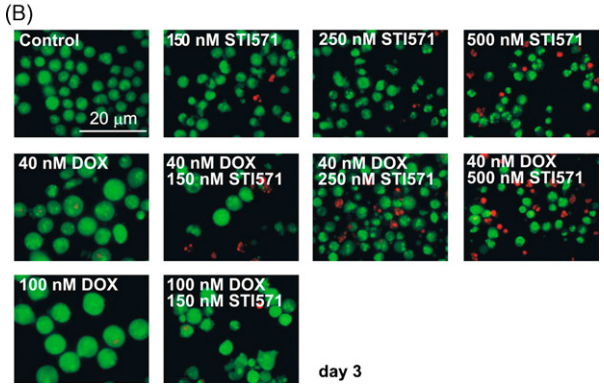

Fig. 4 – Co-treatment with STI571 at low concentrations and DOX (40–100 nM) induces more apoptosis than either drug alone. (A) K562 cells were treated with the indicated concentrations of STI571 and DOX for 2 days, and the percentages of apoptotic cells were determined by Annexin V/propidium iodide staining followed by FACS. Selected histograms from one typical experiment are presented. Values of 3 independent experiments are depicted as bars and means are presented in attached table. (B) Double staining of K562 cells following exposure to DOX or/and STI571 at indicated concentrations. Cells were exposed to drugs for 3 days, and stained with fluorochromes: membrane-permeable acridine orange and impermeable ethidium bromide. Representative microscopic fields are shown. Viable cells had bright green chromatin with organized structure. In early apoptotic cells, the chromatin was condensed or fragmented but still stained green. In late apoptotic cells, it was condensed or fragmented and stained orange, and necrotic cells had bright orange chromatin with organized structure. Quantitative data are presented in Table 1. (For interpretation of the references to color in this figure legend, the reader is referred to the web version of the article.)

were also visible after PI staining. In the control cultures, the majority of cells exhibited high $\Delta\Psi_m$ and was viable (no PI staining). In STI571-treated cultures, $\Delta\Psi_m$ was decreased in concentration-dependent manner (Fig. 6A).

Exposure to STI571 and/or DOX did not immediately result in $\Delta\Psi_m$ dissipation, instead there was a variable latency period after which $\Delta\Psi_m$ started to decrease (Fig. 6B). In K562 cells treated with 150 nM STI571, loss of $\Delta\Psi_m$ started on day 3, whereas with 250 nM STI571 on day 2, but still in both cases the majority of cells retained high $\Delta\Psi_m$. K562 cells treated with 500 nM STI571 were distributed to all three cell populations on day 2, but almost exclusively showed very low $\Delta\Psi_m$ on day 3. Combined treatment with STI571 and DOX markedly enhanced this process. Results are summarized in Fig. 6C. Surprisingly, $\Delta\Psi_m$ dissipation was observed not only for apoptosis-inducing conditions but also in cells exposed to DOX alone. More than 45% of K562 cells incubated with 100 nM DOX exerted low $\Delta\Psi_m$.

This result prompted us to investigate whether changes in $\Delta\Psi_m$ could occur in the conditions optimal for differentiation induced by STI571 or DOX alone or in combination (Fig. 7A). We applied drug concentrations which gave the highest level of benzidine-positive cells (Fig. 3), and the highest relative expression of γ-globin gene. In addition to day 3, $\Delta\Psi_m$ was analyzed on day 4 when differentiation was assessed. $\Delta\Psi_m$ dissipation was observed in 100 nM DOX-treated cells. PI staining (panel b) was very low indicating that loss of $\Delta\Psi_m$ was not connected to the disruption of plasma membrane integrity. In contrast to DOX, STI571 at the concentration optimal for differentiation did not markedly change $\Delta\Psi_m$. In this case, the observed reduction of $\Delta\Psi_m$ was rather related to cell death observed on day 4 (PI staining).

3.7. *DOX but not STI571 induces differentiation in a caspase-dependent manner*

To analyze caspase involvement in erythroid-like differentiation induced by STI571 or DOX, we applied caspase inhibitors. We used the optimal concentrations of drugs alone or in combination to stimulate differentiation of K562 cells and simultaneously one of caspase inhibitors, either a general caspase inhibitor zVAD-fmk, or another one specific for

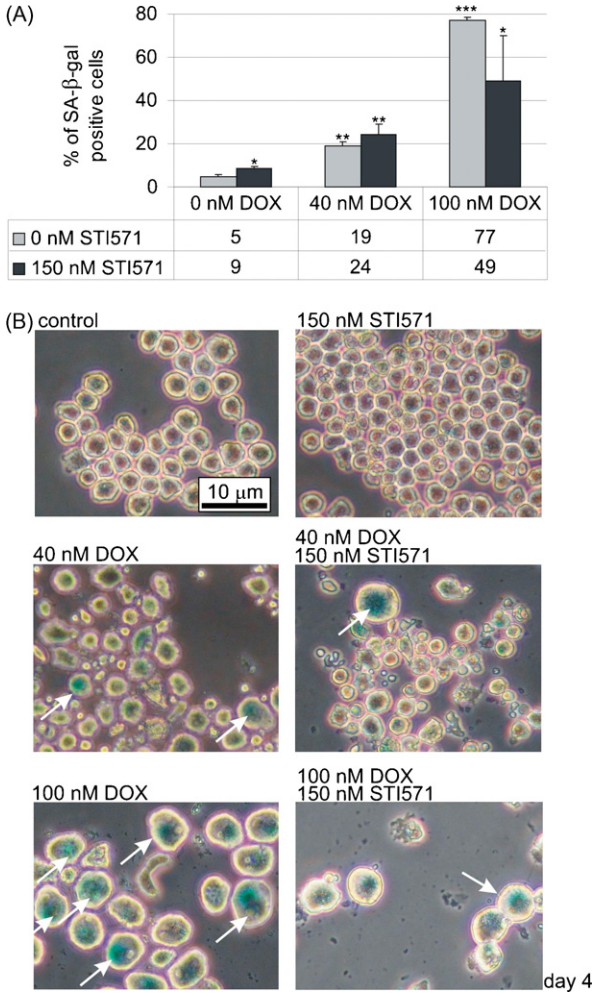

Fig. 5 – DOX but not STI571 induces senescence in K562 cells. (A) Expression of senescence-associated β-galactosidase (SA-β-gal) in K562 cells following 3 days exposure to DOX and/or STI571. Ten different microscopic fields were randomly selected for counting about 200 cells. The percentage of cells with blue color was then calculated. Results from three independent experiments were averaged. 60 nM DOX caused similar level of SA-β-gal-positive cells as 100 nM DOX (not shown). (B) Cells were treated with DOX and/or STI571 at indicated concentrations for 4 days. Representative microscopic fields are shown. Arrows indicate examples of cells with SA-β-gal expression. Blue staining and substantial increase in cellular volume is visible in the case of DOX-treated cells. (For interpretation of the references to color in this figure legend, the reader is referred to the web version of the article.)

caspase-3, zDEVD-fmk. Neither DMSO vehicle nor caspase inhibitors were toxic to the K562 cells or increased cell viability (not shown). They did not influence the differentiation level of K562 cells as well. A marked reduction of differentiation in the presence of caspase inhibitors measured as the percentage of benzidine positive cells was observed in DOX-treated but not in STI571-treated K562 cells (Table 2). Similar results were obtained when the decrease in γ-globin expression was assessed by real-time PCR. When γ-globin expression in K562 cells cultured simultaneously with 60 nM DOX and zDEVD-fmk was compared with that in K562 cells cultured in the presence of DMSO vehicle, a 0.84 ± 0.07-fold change was observed. No difference in the level of γ-globin expression was registered for 150 nM STI571-stimulated K562 cells with or without zDEVD-fmk.

In the following experiments we used a cell membrane-permeable fluorogenic NucView™ 488 Caspase-3 substrate for detecting caspase-3 activity within cells. This compound consists of a fluorogenic DNA dye and a DEVD substrate moiety recognized by caspase-3. DNA dye released by active caspase-3 migrates to the nucleus to stain it green. As expected, in apoptosis-inducing conditions (1 μM STI571 for 3 days) high caspase-3 activity was detected (not shown). That phenomenon was also observed in K562 cells stimulated for 4 days with 100 nM DOX but not with 150 nM STI571 (Fig. 7B). DOX-enlarged cells had their nuclei stained green. We have found these results as supporting the notion that caspase activity induced by 100 nM DOX could participate in differentiation of K562 cells. To further confirm the relationship between caspase activation and differentiation occurring in K562 cells treated with DOX, expression of GPA, a marker of erythroid differentiation was assessed simultaneously with caspase-3 activation. Exposure of K562 cells to 100 nM DOX markedly increased the percentage of GPA/caspase-3 double-positive cells after 4 days of culturing as measured by flow cytometry (Fig. 7C). It raised from about 1% in control to about 35% in DOX-treated cells. An increase in percentage of caspase-3 positive cells, both GPA positive and negative, from about 5% to about 68% suggests that caspase activation preceded erythroid differentiation. Combined treatment with 150 nM STI571 and 15 nM DOX caused an appearance of green-stained fragmented nuclei present mainly in small cells not those enlarged by DOX treatment (Fig. 7B) suggesting rather induction of apoptosis than differentiation. The other process stimulated by DOX, senescence, was not inhibited by caspase inhibitor, zVAD-fmk (Fig. 7D).

4. Discussion

The attempt to eliminate cancer cells requires the understanding of cellular response that is induced by anticancer drugs. K562 cell line derived from a patient in blast crisis is commonly accepted as a cellular model of advanced phase of CML [18,23]. It is apoptosis reluctant mainly due to the constitutive Bcr-Abl activity. Therefore, it represents an appropriate model to investigate the cellular response to cytotoxic drugs after gradual diminishing Bcr-Abl activity.

The current work addresses the combined effects of continuous exposure of K562 cells to various concentrations of STI571, an agent modulating Bcr-Abl activity in a highly specific way, and low concentrations of DOX, a chemotherapeutic drug which has a wide range of cellular targets [11,12]. CI equation chosen for drugs with independent mode of action has shown a broad range of additive collaboration between STI571 and DOX in inhibiting cellular proliferation (Fig. 1B). Comparison of cytotoxic and cytostatic effects revealed that

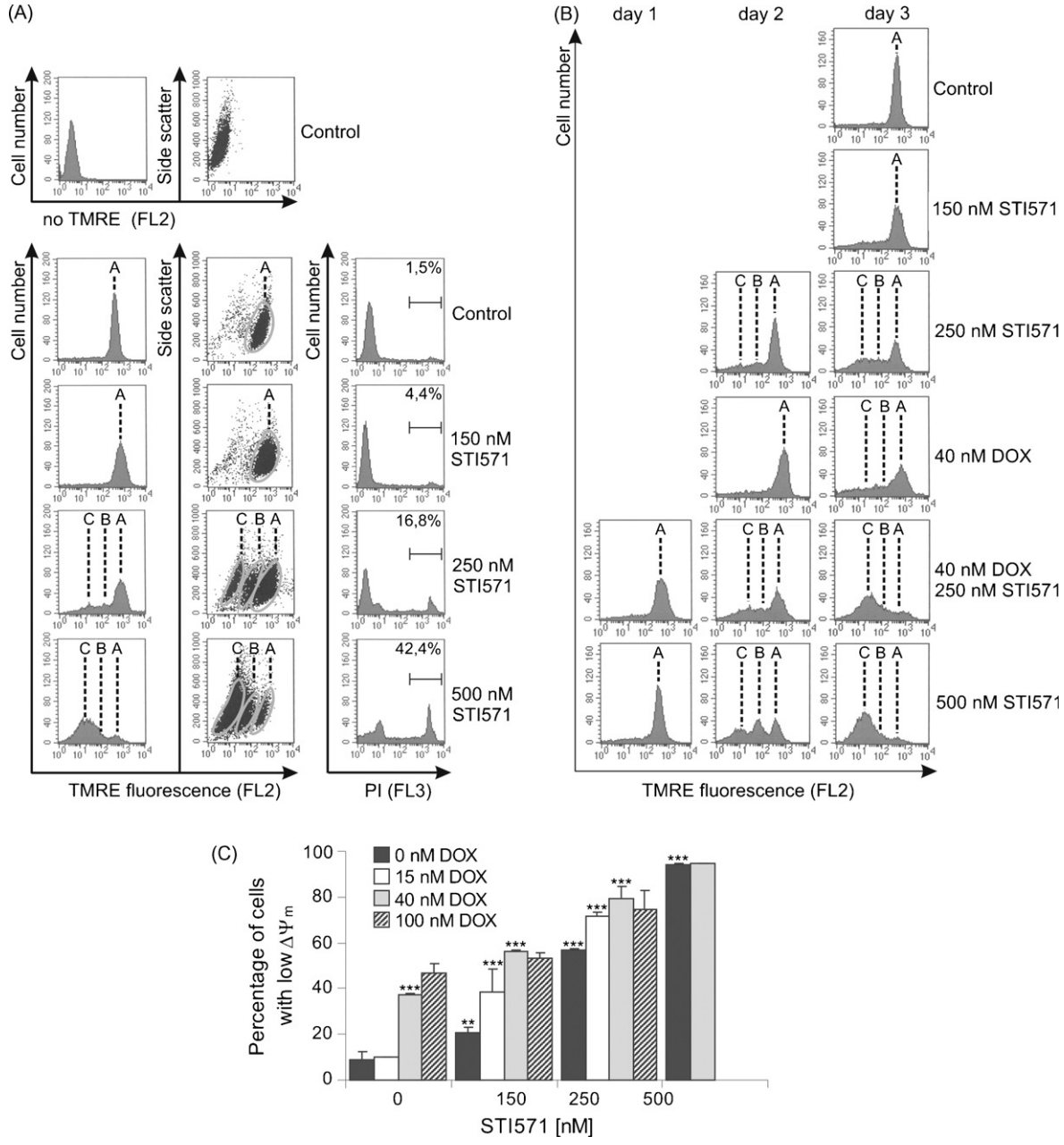

Fig. 6 – Loss of mitochondrial transmembrane potential (Ψ_m) is observed in STI571 and DOX-treated cells. K562 cells were treated with 40 nM DOX alone or in combination with STI571 at the indicated concentrations, stained with TMRE and analyzed by flow cytometry. Reduced fluorescence intensity compared to that of the control indicates a decline in mitochondrial membrane potential. (A) Representative histograms obtained for STI571-treated cells after 3 days. Three cell populations could be distinguished. Population A consisted of cells with polarized mitochondria with high $\Delta\Psi_m$ where TMRE was accumulated (>2×10^2), population B of cells with decreased $\Delta\Psi_m$, and population C of cells with very low $\Delta\Psi_m$. Density plots of TMRE fluorescence versus side scatter (SSC) show the corresponding populations (outline in gray). In parallel, a plasma membrane integrity was assessed by PI staining. (B) Representative histograms of cells treated with STI571 and/or DOX for 1–3 days. (c) Quantitative results of FACS of TMRE loaded cells after 3 days of treatment with STI571 and/or DOX. Data are expressed as percentage of cells with low TMRE fluorescence intensity defined as below 2×10^2. Data represent means and standard deviation of 3 independent experiments.

cell death defined as loss of cell membrane integrity was not the major cause of reduced proliferation when STI571 at the concentrations of 250 nM or lower was used alone or in combination with DOX.

To explain growth arrest without cytotoxic effect, differentiation and senescence were considered. Differentiation of K562 cells can be induced by a variety of chemical compounds as diverse as hydroxyurea, cisplatin, butyrate, and ara-C

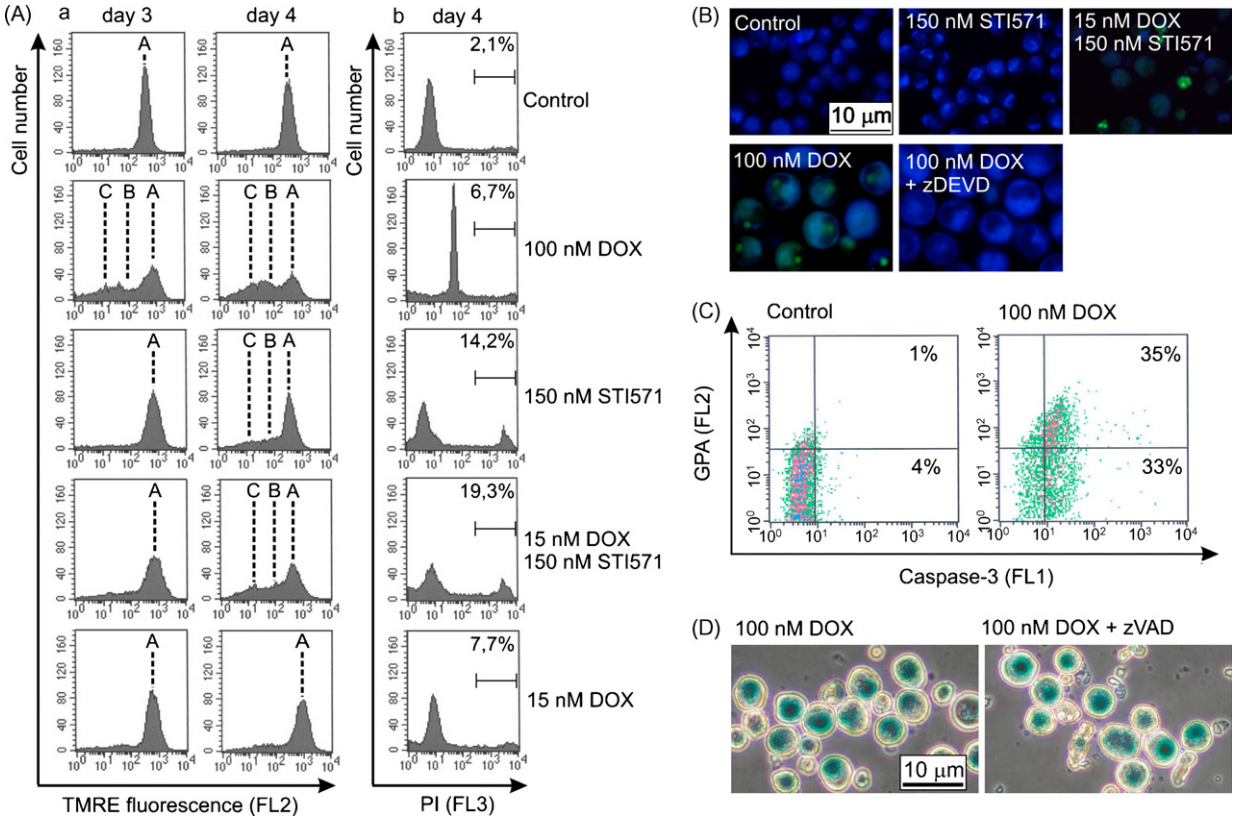

Fig. 7 – $\Delta\Psi_m$ dissipation and caspase-3 activation in conditions optimal for differentiation. (A) K562 cells were treated with DOX and/or STI571 at indicated concentrations for 3 or 4 days. Representative histograms after TMRE or PI staining are shown. Only 100 nM DOX markedly reduced $\Delta\Psi_m$ with no effect on cellular viability. The peak of PI-negative cells after DOX treatment was shifted rightward due to fluorescence caused by this drug itself, which was also observed in other histograms (compare with Fig. 4A). (B) Caspase-3 activity was present in K562 cells treated with 100 nM DOX or with combination of 150 nM STI571 and 15 nM DOX but not with 150 nM STI571 alone or in untreated cells. NucView™ 488 Caspase-3 substrate was applied to detect caspase-3 activity as described in Section 2. Adding caspase-3 inhibitor Ac-DEVD-CHO prior to NucView™ 488 Caspase-3 substrate completely abolish caspase-3 activity present in 100 nM DOX-treated cells. (C) K562 cells were treated with 100 nM DOX for 4 days, and the percentages of GPA/caspase-3 double-positive cells and caspase-3 positive cells were determined by FACS. The results are from a single typical experiment. (D) Caspase inhibitor zVAD-fmk did not affect senescence induced by 100 nM DOX. Two experiments were performed and representative microscopic fields are shown.

[24–27]. Also STI571 [28,29] and DOX [18,21,30,31] can stimulate differentiation of K562 cells. The involvement of p38 MAP kinase pathway was shown for some of those stimuli including STI571 [23,26,28]. But still it remains unclear how so diverse agents can trigger differentiation of a CML cell line. Exposure of cells to inhibitors of caspases together with STI571 or DOX at concentrations inducing the highest rate of differentiation indicated that different mechanisms were executed by STI571 and DOX to trigger differentiation. STI571 induced differentiation in caspase-independent manner, since neither a general inhibitor of caspases, zVAD-fmk nor a caspase-3 inhibitor, zDEVD-fmk influenced the level of differentiated cells (Table 2). This lack of caspase involvement in STI571-mediated differentiation confirmed recently published findings that STI571-mediated apoptosis and differentiation are fully unrelated processes and can be distinguished on the basis of their caspase dependence [32]. The inhibitor of caspases, zVAD-fmk was found to abolish STI571-induced apoptosis but not differentiation which was also unaffected by shRNAi silencing of caspase-3. Our current results clearly indicated that differentiation induced by DOX, in contrast to STI571, involves caspases (Table 2, Fig. 7B). This process is accompanied by a significant decrease in mitochondrial transmembrane potential ($\Delta\Psi_m$) (Fig. 7A) but is not connected to cell death. Although there is compelling evidence that activation of caspases via a mitochondrion-dependent pathway is implied in non-apoptotic differentiation programs [15,33,34], our study indicates that also an anticancer agent such as DOX can stimulate this mechanism to some extent. Hence, our data support the notion that chemically induced differentiation in cancer cells can be dependent (as for DOX) or independent (as for STI571) on caspase activity.

In the previous report, we have shown that DOX stimulates GATA-1 activity [21]. This transcription factor positively regulates erythroid and anti-apoptotic genes and it is protected by the heat shock protein 70 (Hsp70) from

Table 2 – Caspase-dependence of erythroid-like differentiation of K562 cells

	Fold change in the percentage of benzidine-positive cells caused by caspase inhibitors:	
	zVAD-fmk	zDEVD-fmk
Control	0.91 ± 0.01 (1.8/2.0)	0.95 ± 0.01 (1.8/1.9)
DMSO	1.04 ± 0.01 (2.2/2.1)	0.95 ± 0.01 (2.5/2.6)
60 nM DOX	0.69 ± 0.01 (12.7/18.4)	0.81 ± 0.02 (16.0/19.7)
100 nM DOX	0.69 ± 0.02 (26.3/38.3)	Not determined
150 nM STI571	0.97 ± 0.08 (26.9/27.7)	1.01 ± 0.06 (28.9/28.6)
250 nM STI571	0.98 (15.4/15.7)	0.96 (20.9/21.7)

K562 cells were cultured simultaneously with DOX or STI571 at indicated concentrations, and one of caspase inhibitors zVAD-fmk or zDEVD-fmk at the final concentration of 40 μM or with a carrier (DMSO). Benzidine assay was done on day 4 as described in Section 2. Fold decrease in the percentage of benzidine-positive cells caused by caspase inhibitors was then calculated. The average values of percentage of benzidine positive cells estimated in the presence (first value) or absence (second value) of caspase inhibitors are shown in brackets. Except for cells treated with 250 nM STI571, results from three independent experiments were averaged and standard deviation was calculated.

caspase-3-mediated cleavage during erythropoiesis [34]. Since Bcr-Abl expressing K562 cells display high endogenous levels of Hsp70 [35], we could postulate that this chaperone protein might secure differentiation when GATA-1 and caspase-3 activities are simultaneously induced by DOX. It could also contribute to Bcr-Abl-mediated resistance to apoptosis unless Bcr-Abl tyrosine activity is inhibited by STI571.

Our results not only clearly indicate that DOX-dependent caspase activity can participate in the induction of erythroid-like differentiation but they also show that this can decrease apoptosis-inducing concentration of STI571 in combined treatment. It has been already demonstrated that STI571 can independently trigger both differentiation and apoptosis in K562 cells [29,32]. Our current study provides a more detailed analysis of cellular response to STI571 in the range of concentrations where the switch between differentiation and apoptosis is observed (Fig. 8). At low concentrations, STI571 predominantly induces cell differentiation, while at higher concentrations it predominantly triggers apoptosis. By combining STI571 with DOX, an enhancement of both processes was observed in narrow ranges of drug concentrations (Fig. 8). The significant increase in the percentage of apoptotic cells observed when 40–100 nM DOX was combined with non-apoptotic concentration of STI571 (150 nM) can be explained by the raise of active caspases to the level sufficient to induce the apoptotic program. Evidence of apoptotic cell death for 150 nM STI571 combined with DOX was obtained at concentration as low as 15 nM when NucView™ 488 Caspase-3 substrate was used (Fig. 7B).

Our results might also be related to the observations published for differentiation processes naturally occurring in many cell types. It has been shown for lens cell differentiation that pro-survival factors allow pro-apoptotic molecules to function as molecular switches in the differentiation process without moving the balance toward apoptosis [14]. In erythropoiesis, Bcl-X_L is such a key survival factor and its upregulation is mediated by GATA-1 and erythropoietin [34,36]. In K562 cell line which is derived from CML in blast crisis, Bcl-X_L is overexpressed due to the constitutive activity of Bcr-Abl [37]. Lower levels of Bcl-X_L found in patients in chronic phase of CML were associated with a higher differentiation rate [38]. Therefore, our data suggest that STI571 depending on its concentration might decrease Bcr-Abl activity and subsequently the expression of Bcl-X_L either to a level which is still high enough to support survival of DOX and/or STI571-differentiated cells or to the level which is not sufficient to prevent the massive release of

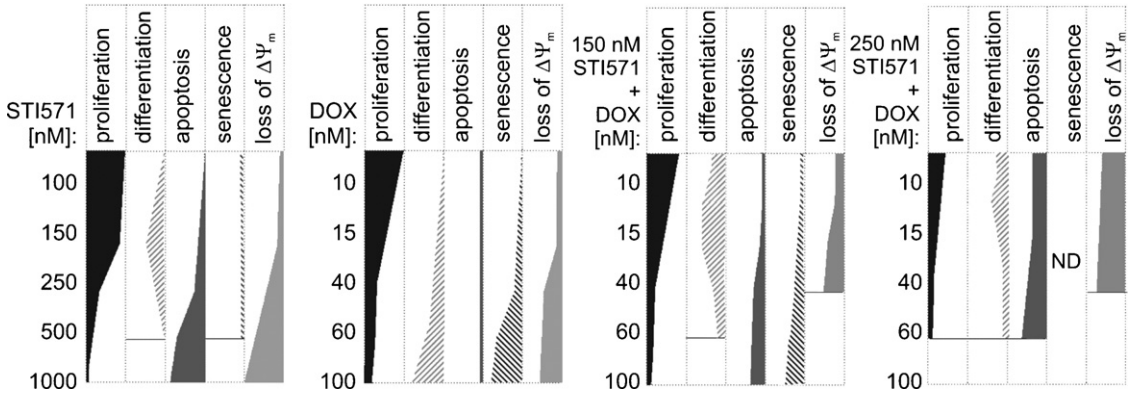

Fig. 8 – Schematic presentation of contribution of cellular processes such as differentiation, apoptosis and senescence to reduced proliferation caused by low concentrations of DOX and STI571 used alone or in combination. $\Delta\Psi_m$ dissipation is included. The width of the rectangles corresponds to 100% except for differentiation where it is 50%. STI571 depending on its concentration induces differentiation or apoptosis but only the latter process could be related to loss of $\Delta\Psi_m$. DOX alone induces differentiation and senescence in a concentration-dependent manner, which is accompanied by $\Delta\Psi_m$ dissipation. Drugs used in combination enhance differentiation or apoptosis in narrow ranges of concentrations. A decrease in the levels of senescence and differentiation is observed in apoptosis-inducing conditions. The loss of mitochondrial transmembrane potential ($\Delta\Psi_m$) is enhanced by combined treatment. A cumulative caspase activation by DOX and STI571 is hypothesized to be responsible for decreasing the apoptotic-effective concentration of STI571 (see text for further explanation).

pro-apoptotic molecules from mitochondria to the cytosol (Fig. 8).

Besides differentiation, DOX can also induce senescence in a variety of cancer cell types [39,40]. This long-term arrest could be characterized by increased expression of senescence marker SA-β-gal and some phenotypic features such as cell enlargement and increased granularity which were observed for DOX-treated cells also in our study. The senescence program could be either p53-dependent or independent [39]. K562 cells do not have a functional p53 and therefore our data suggest that p53 is not necessary to induce senescence in this cell line. Similar observations were reported in hematopoietic stem cells [41] and normal diploid WI38 fibroblasts [42] upon treatment with busulfan. The relation between differentiation and senescence, both observed in DOX-treated CML cells needs to be further explored.

In summary, the principal findings of our study performed in human K562 cell line indicate that: (i) DOX and STI571 additively affect cellular proliferation; (ii) DOX and STI571 used at low concentrations induce differentiation but only DOX induces that process in a caspase-dependent manner; (iii) apoptosis triggered by STI571 and differentiation caused by DOX is accompanied by mitochondrial transmembrane potential dissipation; (iv) cellular fate, either differentiation, senescence, or apoptosis, depends on concentrations of either drug; (v) DOX-induced caspase activity could be a causal factor for a decrease in the apoptotic-effective concentration of STI571.

Our study extends the understanding of the effects observed in an apoptosis-reluctant CML cell line after treatment with STI571 combined with chemotherapeutics. We can speculate that by combining the effects of STI571 with induction of differentiation and senescence, an enhancement in elimination of cancer cells could be obtained. Much lower than pharmacologically achievable STI571 concentrations were highly effective in inducing apoptosis when used with low concentrations of DOX. We consider those conditions as attractive for a clinical study for at least three reasons: firstly, because drugs can be sustained at rather low concentrations in patients undergoing anticancer therapy and secondly, lowering drug concentrations could further decrease toxicity, and finally, induction of differentiation and/or senescence in cancer cells could reduce the possibility of cancer relapse. But whether this *in vitro* combinatorial activity will translate into better response and survival rates of CML patients must be proven in clinical trails.

Acknowledgments

The authors wish to thank Dr. Markus Düchler for stimulating discussions and helpful comments, Dr. Irena Oszczapowicz and Mrs. Malgorzata Wasowska for DOX synthesis, Prof. Janusz Blasiak for supplying STI571. We are grateful to Dr. Marta Stasiak for her help in FACS and Mrs. Grazyna Kus for a technical work. This research was supported by Grant N401 116 31/2630 from the Ministry of Scientific Research and Higher Education and by Grant 502-11-602 from Medical University of Lodz.

REFERENCES

[1] Druker BJ, Tamura S, Buchdunger E, Ohno S, Segal GM, Fanning S, et al. Effects of a selective inhibitor of the Abl tyrosine kinase on the growth of Bcr-Abl positive cells. Nat Med 1996;2:561–6.
[2] Mauro MJ, Deininger MW. Chronic myeloid leukemia in 2006: a perspective. Haematologica 2006;91:152–8.
[3] Rowe JM. Closing the gap in CML. Blood 2007;109:2271.
[4] Litzow MR. Imatinib resistance: obstacles and opportunities. Arch Pathol Lab Med 2006;130:669–79.
[5] Tauchi T, Ohyashiki K. The second generation of BCR-ABL tyrosine kinase inhibitors. Int J Hematol 2006;83:294–300.
[6] Thiesing JT, Ohno-Jones S, Kolibaba KS, Druker BJ. Efficacy of STI571, an abl tyrosine kinase inhibitor, in conjunction with other antileukemic agents against bcr-abl-positive cells. Blood 2000;96:3195–9.
[7] Yu C, Krystal G, Varticovksi L, McKinstry R, Rahmani M, Dent P, et al. Pharmacologic mitogen-activated protein/extracellular signal-regulated kinase kinase/mitogen-activated protein kinase inhibitors interact synergistically with STI571 to induce apoptosis in Bcr/Abl-expressing human leukemia cells. Cancer Res 2002;62:188–99.
[8] Liu WM, Stimson LA, Joel SP. The in vitro activity of the tyrosine kinase inhibitor STI571 in BCR-ABL positive chronic myeloid leukaemia cells: synergistic interactions with anti-leukaemic agents. Br J Cancer 2002;86:1472–8.
[9] Yin T, Wu YL, Sun HP, Sun GL, Du YZ, Wang KK, et al. Combined effects of As4S4 and imatinib on chronic myeloid leukemia cells and BCR-ABL oncoprotein. Blood 2004;104:4219–25.
[10] Du Y, Wang K, Fang H, Li J, Xiao D, Zheng P, et al. Coordination of intrinsic, extrinsic, and endoplasmic reticulum-mediated apoptosis by imatinib mesylate combined with arsenic trioxide in chronic myeloid leukemia. Blood 2006;107:1582–90.
[11] Gewirtz DA. A critical evaluation of the mechanisms of action proposed for the antitumor effects of the anthracycline antibiotics adriamycin and daunorubicin. Biochem Pharmacol 1999;57:727–41.
[12] Minotti G, Menna P, Salvatorelli E, Cairo G, Gianni L. Anthracyclines: molecular advances and pharmacologic developments in antitumor activity and cardiotoxicity. Pharmacol Rev 2004;56:185–229.
[13] Schwerk C, Schulze-Osthoff K. Non-apoptotic functions of caspases in cellular proliferation and differentiation. Biochem Pharmacol 2003;66:1453–8.
[14] Weber GF, Menko AS. The canonical intrinsic mitochondrial death pathway has a non-apoptotic role in signaling lens cell differentiation. J Biol Chem 2005;280:22135–4.
[15] Lamkanfi M, Festjens N, Declercq W, Vanden Berghe T, Vandenabeele P. Caspases in cell survival, proliferation and differentiation. Cell Death Differ 2007;14:44–55.
[16] Zermati Y, Garrido C, Amsellem S, Fishelson S, Bouscary D, Valensi F, et al. Caspase activation is required for terminal erythroid differentiation. J Exp Med 2001;193:247–54.
[17] Fernando P, Megeney LA. Is caspase-dependent apoptosis only cell differentiation taken to the extreme? Federation Am Societies Exp Biol J 2007;21:8–17.
[18] Czyz M, Szulawska A, Bednarek AK, Duchler M. Effects of anthracycline derivatives on human leukemia K562 cell growth and differentiation. Biochem Pharmacol 2005;70:1431–42.
[19] Chou TC, Talalay P. Quantitative analysis of dose-effect relationships: the combined effects of multiple drugs or enzyme inhibitors. Adv Enzyme Regul 1984;22:27–55.

[20] Chou TC, Motzer RJ, Tong Y, Bosl GJ. Computerized quantitation of synergism and antagonism of taxol, topotecan, and cisplatin against human teratocarcinoma cell growth: a rational approach to clinical protocol design. J Natl Cancer Inst 1994;86:1517–24.
[21] Szulawska A, Arkusinska J, Czyz M. Accumulation of gamma-globin mRNA and induction of irreversible erythroid differentiation after treatment of CML cell line K562 with new doxorubicin derivatives. Biochem Pharmacol 2007;73:175–84.
[22] Pfaffl MW, Horgan GW, Dempfle L. Relative expression software tool (REST) for group-wise comparison and statistical analysis of relative expression results in real-time PCR. Nucleic Acids Res 2002;30:e36.
[23] Jacquel A, Herrant M, Legros L, Belhacene N, Luciano F, Pages G, et al. Imatinib induces mitochondria-dependent apoptosis of the Bcr-Abl-positive K562 cell line and its differentiation toward the erythroid lineage. Federation Am Societies Exp Biol J 2003;17:2160–2.
[24] Park JI, Choi HS, Jeong JS, Han JY, Kim IH. Involvement of p38 kinase in hydroxyurea-induced differentiation of K562 cells. Cell Growth Differ 2001;12:481–6.
[25] Bianchi N, Ongaro F, Chiarabelli C, Gualandi L, Mischiati C, Bergamini P, et al. Induction of erythroid differentiation of human K562 cells by cisplatin analogs. Biochem Pharmacol 2000;60:31–40.
[26] Witt O, Sand K, Pekrun A. Butyrate-induced erythroid differentiation of human K562 leukemia cells involves inhibition of ERK and activation of p38 MAP kinase pathways. Blood 2000;95:2391–6.
[27] Cortesi R, Gui V, Gambari R, Nastruzzi C. In vitro effect on human leukemic K562 cells of co-administration of liposome-associated retinoids and cytosine arabinoside (Ara-C). Am J Hematol 1999;62:33–43.
[28] Kohmura K, Miyakawa Y, Kawai Y, Ikeda Y, Kizaki M. Different roles of p38 MAPK and ERK in STI571-induced multi-lineage differentiation of K562 cells. J Cell Physiol 2004;198:370–6.
[29] Kuzelova K, Grebenova D, Marinov I, Hrkal Z. Fast apoptosis and erythroid differentiation induced by imatinib mesylate in JURL-MK1 cells. J Cell Biochem 2005;95:268–80.
[30] Jeannesson P, Lahlil R, Chenais B, Devy L, Gillet R, Aries A, et al. Anthracycline as tumor cell differentiating agents: effects on the regulation of erythroid gene expression. Leuk Lymphoma 1997;26:575–87.
[31] Morceau F, Aries A, Lahlil R, Devy L, Jardillier JC, Jeannesson P, et al. Evidence for distinct regulation processes in the aclacinomycin- and doxorubicin-mediated differentiation of human erythroleukemic cells. Biochem Pharmacol 1996;51:839–45.
[32] Jacquel A, Colosetti P, Grosso S, Belhacene N, Puissant A, Marchetti S, et al. Apoptosis and erythroid differentiation triggered by Bcr-Abl inhibitors in CML cell lines are fully distinguishable processes that exhibit different sensitivity to caspase inhibition. Oncogene 2007;26:2445–58.
[33] Launay S, Hermine O, Fontenay M, Kroemer G, Solary E, Garrido C. Vital functions for lethal caspases. Oncogene 2005;24:5137–48.
[34] Ribeil JA, Zermati Y, Vandekerckhove J, Cathelin S, Kersual J, Dussiot M, et al. Hsp70 regulates erythropoiesis by preventing caspase-3-mediated cleavage of GATA-1. Nature 2007;445:102–5.
[35] Guo F, Sigua C, Bali P, George P, Fiskus W, Scuto A, et al. Mechanistic role of heat shock protein 70 in Bcr-Abl-mediated resistance to apoptosis in human acute leukemia cells. Blood 2005;105:1246–55.
[36] Gregory T, Yu C, Ma A, Orkin SH, Blobel GA, Weiss MJ. GATA-1 and erythropoietin cooperate to promote erythroid cell survival by regulating bcl-xL expression. Blood 1999;94:87–96.
[37] Horita M, Andreu EJ, Benito A, Arbona C, Sanz C, Benet I, et al. Blockade of the Bcr-Abl kinase activity induces apoptosis of chronic myelogenous leukemia cells by suppressing signal transducer and activator of transcription 5-dependent expression of Bcl-xL. J Exp Med 2000;191:977–84.
[38] Gutiérrez-Castellanos S, Cruz M, Rabelo L, Godínez R, Reyes-Maldonado E, Riebeling-Navarro C. Differences in BCL-X(L) expression and STAT5 phosphorylation in chronic myeloid leukaemia patients. Eur J Haematol 2004;72:231–8.
[39] Chang BD, Broude EV, Dokmanovic M, Zhu H, Ruth A, Xuan Y, et al. A senescence-like phenotype distinguishes tumor cells that undergo terminal proliferation arrest after exposure to anticancer agents. Cancer Res 1999;59:3761–7.
[40] Jackson JG, Pereira-Smith OM. Primary and compensatory roles for RB family members at cell cycle gene promoters that are deacetylated and downregulated in doxorubicin-induced senescence of breast cancer cells. Mol Cell Biol 2006;26:2501–10.
[41] Meng A, Wang Y, Van Zant G, Zhou D. Ionizing radiation and busulfan induce premature senescence in murine bone marrow hematopoietic cells. Cancer Res 2003;63:5414–9.
[42] Probin V, Wang Y, Bai A, Zhou D. Busulfan selectively induces cellular senescence but not apoptosis in WI38 fibroblasts via a p53-independent but extracellular signal-regulated kinase-p38 mitogen-activated protein kinase-dependent mechanism. J Pharmacol Exp Ther 2006;319:551–60.